SECOND EUROPEAN CONFERENCE ON EARTHQUAKE ENGINEERING AND SEISMOLOGY, ISTANBUL AUG. 25-29, 2014

SEISMIC ASSESSMENT OF EXISTING CHEVRON BRACED FRAMES DESIGNED IN ACCORDANCE WITH THE 1980 CANADIAN CODE REQUIREMENTS

Yasaman BALAZADEH MINOUEI[1], Sanda KOBOEVIC[2] and Robert TREMBLAY[3]

ABSTRACT

The seismic deficiencies of a 10-storey steel braced frame located in Vancouver, British Columbia, designed in accordance with the 1980 National Building Code of Canada and the CSA-S16.1-M78 steel design standard were evaluated using the nonlinear procedure defined in the ASCE 41-13 standard. Nonlinear time-history analysis of the tension-compression chevron-braced frame was performed for a set of seven historical ground motion records compatible with the NBCC design spectrum. When the inelastic response of braces was represented in the model, buckling of the braces was predicted at the lower levels of the structure. Beam buckling at the lower levels of the building was observed when inelastic beam response was included in the model. Beam buckling in chevron braced frames is further investigated using different types of analytical models.

INTRODUCTION

The seismic design provisions were introduced in the National Building Code of Canada (NBCC) in 1941 (Mitchell et al., 2010). Seismic design and detailing provisions for steel structures were integrated into the CSA S16 design standard in 1989. In previous editions of CSA S16, ductile behaviour was not explicitly taken into account in seismic design. As the understanding of seismic behaviour gradually increased over the years based on experiences from past earthquakes and extensive research studies, design provisions have been continuously updated (Tremblay 2011). The latest Canadian building code, NBCC 2010 (NRCC 2010), and steel design standard CSA S16-09 (CSA 2009) reflect the most recent findings in the area of seismic engineering and are comparable to seismic design norms of other countries.

In the 1980's, prior to the implementation of seismic requirements in CSA S16, steel braced frames with tension-only bracing and chevron bracing systems were the most common types of lateral load resisting system used in steel buildings in Canada. The bracing members were usually made of back-to-back double angle sections while beams and columns were selected from W-shaped sections. At the brace ends, back-to-back legs were connected to single vertical gusset plates using high strength bolts. Steel concentrically braced frames designed in accordance with the provisions of the 1980 NBCC (NRCC 1980) and the CSA-S16.1-M78 steel design standard (CSA 1978) are likely to exhibit severe seismic deficiencies due to the absence of any explicit consideration of special seismic detailing

[1] Graduate student, Ecole Polytechnique of Montreal, Montreal, yasaman.balazadeh-minouei@polymtl.ca
[2] Assistant Professor, Ecole Polytechnique of Montreal, Montreal, sanda.koboevic@polymtl.ca
[3] Professor, Ecole Polytechnique of Montreal, Montreal, robert.tremblay@polymtl.ca

requirements in their design. The seismic assessment of steel braced frame structures used in a prototype 10-storey building located in Vancouver, British Columbia, was carried out in a previous study (Jiang et al., 2012a). The response of the structure was evaluated using the results of the response spectrum analysis as specified in the NBCC 2010. The resistance of the structural elements and connections was calculated in according with the CSA-S16-09 provisions. The results obtained for tension-compression chevron braced frame showed that none of the structural elements including braces, columns and beams had sufficient capacity. In addition, the brace connections had inadequate strength. The governing failure mode for all brace connections was block shear failure.

In this paper, the seismic response of a tension-compression chevron-braced frame is further studied by conducting the seismic assessment based on results of nonlinear analysis. The structure is assessed following the procedure detailed in the ASCE 41-13 standard (ASCE 2013). This U.S. standard provides requirements for the analysis and assessment of existing buildings and includes acceptance criteria for the structural components. The Tier 3 systematic evaluation procedure is followed to assess the behaviour at the collapse prevention structural performance level for 2% in 50 years hazard, which corresponds to the basic NBCC performance objective in the 2010 NBCC. Member capacities are determined using the provisions of the current CSA S16-09 steel design standard. The structure is analysed using the nonlinear dynamic procedure proposed in the ASCE 41 standard. Different numerical modelling techniques are applied to assess the seismic demand on the structure, and examine the effect of nonlinearity of different structural members on the global seismic response of the building. The nonlinear analysis is carried out for a group of seven historical ground motion records scaled to match the NBCC design spectrum. The study focuses on the response of braces and beams. For the beams, it is found that in-plane buckling could occur. This failure mode has not been investigated in past studies. The response of the beams is further investigated by using five different types of beam models.

DESIGN OF THE BUILDING STUDIED

The plan view and frame elevation of the studied 10-storey building is illustrated in Fig.1. The structure was designed according to the design provisions of the 1980 NBCC and the CSA-S16.1-M78 steel design standard. Because of the large differences between the level of design seismic loads proposed in the NBCC 1980 and those specified in the 2010 NBCC, NBCC 1980 was chosen to design the building. The studied structure is located in Vancouver, British Colombia. It is situated on firm ground site which classifies for foundation factors F = 1.0 (NBCC 1980) or $F_a = F_v$ = 1.0 (NBCC 2010). The importance factor for the building, I, was taken as one. Chevron bracing was used in E-W direction whereas tension-only braced frames with diagonals in the X configuration were selected in the N-S direction. The fundamental period was estimated using the Rayleigh method, as would have been done in practice in the 1980's. The periods of the chevron braced and X-braced frames are 2.00 s and 2.77 s, respectively. The obtained periods are significantly longer than the 0.54 s value calculated using the NBCC empirical expression, $T_{emp} = 0.09h_n/D^{0.5}$where h_n = 40.23 m and D = 45.72 m. The equivalent static force procedure was applied to determine earthquake effects as permitted in NBCC 1980 for regular structures. The seismic base shear of the structure was determined from:

$$V = ASKIFW \tag{1}$$

In this equation, A is the design acceleration ratio, S is the seismic response factor (= $0.5/T^{0.5}$), K is a coefficient calculated based on the type of construction, I is the importance factor, F is the foundation factor and W is the seismic weight. For this study, A = 0.08, I = 1.0, F = 1.0, W = 83756 kN for the entire building, and K = 1.0 and 1.3 for the tension-compression and tension-only bracing, respectively. The resulting seismic force coefficients, V/W, are equal to = 0.029 and 0.032 for the chevron bracing and tension-only bracing systems, respectively. To account for higher mode effects, which are likely to impact the response of this taller building, a concentrated lateral force, F_t = 7.74% V, was applied at the roof level. The remaining seismic load, $V - F_t$, was distributed along the height of the structure as a function of the relative product of the storey seismic weight and height measured

from the ground up to the level under consideration. In-plane torsion and P-delta effects were considered in design. The overturning moment reduction factor, *J*, was taken equal to 1.0.

The frames of the 10-storey building were designed based on the requirements of CSA-S16.1-M78. The structural members were made of CSA-G40.21-300W steel (F_y = 300 MPa, F_u = 450 MPa). All bracing members were double angle sections with equal leg angles in back-to-back position. Class 3 sections were used for the bracing members to control width-to-thickness ratios, as prescribed in CSA-S16.1-M78. For chevron bracing members, the overall slenderness ratio was limited to 200. One stitch was also placed at the mid-length of the bracing members to satisfy the CSA-S16.1-M78 slenderness provision. The back-to-back legs of the angles were connected to single vertical gusset plates using high strength A325 bolts, 19.1 mm in diameter. The design of the bracing members was governed by axial strength requirements, except at the roof level where selection of the braces was governed by maximum brace overall slenderness limits. For these over strong braces, connection design was controlled by the 50% C_r or T_r minimum force requirement, which resulted in beneficial overstrength. CSA S16.1-M78 did not consider shear lag effects and the block shear failure mode for such bolted connections; therefore, the brace connections were smaller compared to current brace connection designs. The beams and columns were selected from W sections, and the columns were tiered in two-storey segments. The beams were assumed to be laterally supported by the floors and thus were selected to resist shear and flexure from gravity loads and strong-axis buckling under combined axial compression and bending.

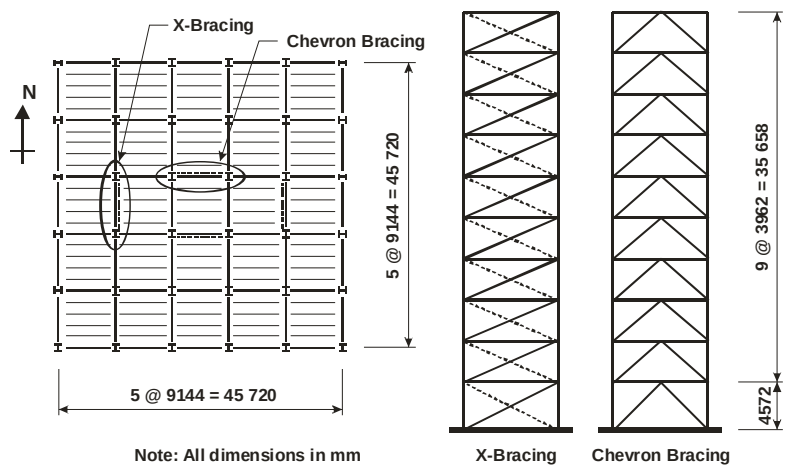

Figure 1. Plan view and braced frame elevations of the 10-storey building

NUMERICAL MODELLING

According to the ASCE 41 standard, a two dimensional model can be used to perform an analysis if the structure has rigid diaphragms and the displacement multiplier due to total torsional moments does not exceed 1.5 at any floor. The displacement multiplier is the ratio of the maximum displacement at any point on the floor diaphragm to the average displacement ($\delta_{max}/\delta_{avg}$). Accidental torsion should be considered in the analysis unless it can be shown that the accidental torsional moment is less than 25% of the inherent torsional moment in the building or the displacement multiplier calculated for the applied loads and accidental torsion is less than 1.1 at every floor. In this study, the maximum value of the displacement multiplier was 1.09. Consequently, it was possible to use a two-dimensional model for the nonlinear analysis and accidental torsion effects could be neglected.

The analytical model of the studied frame was developed in the OpenSees finite element structural analysis platform (McKenna and Fenves 2004). Two modelling approaches, named Model B and Model C, were considered to evaluate the seismic behaviour of the structural members. In Model B, nonlinear beam-column elements were used for the braces whereas elastic beam-column elements were used for the beams and columns. This model permitted partial study of the nonlinear frame response accounting only for the cyclic tensile yielding and inelastic buckling of the braces. Each

brace member was modelled using 16 nonlinear beam-column elements, with 4 integration points per element (Bertero 2004) and fiber discretization of the section to reproduce distributed plasticity. The two series of angle elements were connected at their ends and at the locations of the stitch connectors placed at mid-length of the bracing members. In the connection zone, the double angle sections were linked to each other by means of elastic beam column elements with high axial and flexural stiffness. The connections of the braces to the gusset plates were represented by zero-length elements. To reproduce the nonlinear behaviour of braces, the Giuffré-Menegotto-Pinto (Steel 02) material with kinematic and isotropic hardening properties was assigned to the fibers representing the angle cross-sections. Initial out-of-straightness and residual stresses were also considered (Balazadeh-Minouei et al., 2013; Jiang et al., 2012b). Elastic beam elements were used to model the beams and columns in order to evaluate the elastic force demand on these members. Actual flexural and axial stiffness properties of beams and columns were assigned to the beam-column elements and a zero-length element with high axial stiffness and negligible flexural stiffness was considered to model the beam-column connections. Column bases were assumed to be pinned.

In Model C, nonlinear beam-column elements were used for both the braces and the beams. The columns were represented by elastic beam elements. Similarly to the braces in Model B, 16 nonlinear beam-column elements with 4 integration points placed along each element were used for the beam members. The cross section of each element was discretized by fibers to which the Steel02 material was assigned with a residual stress pattern typical for W shaped sections. Hence, beam inelastic buckling response and its effects on the braced frame response could be examined. The beams were assumed to be laterally supported, thus only in-plane flexural buckling was represented. Beam initial in-plane out-of-straightness was assigned in the form of two half-sine waves having maximum amplitude of 1/1000 of half the total beam length. This amplitude corresponds to the fabrication tolerances specified in CSA-S16.1-M78. The inelastic out-of-plane flexural response of the beam-to-brace gusset plate connections was modelled using zero-length elements with fiber discretization and Steel 02 inelastic material properties. Residual stresses were not modelled in the gusset plates.

The load combination including gravity load and earthquake effects as specified in the NBCC was used in the analyses , i.e. 1.0D+0.5L+0.25S+1.0E, where D, L, S and E respectively refer to the dead load, the floor live load, the roof snow load and the earthquake load. To simulate P-Delta effects in the analyses, a leaning column carrying gravity loads was linked to the braced frame model.

GROUND MOTIONS

Twenty pairs of two horizontal components of historical ground motions were initially selected considering the magnitude-distance scenarios that contribute the most to the seismic hazard at the site, as proposed by Atkinson (2009). Out of these records, seven pairs of ground motion time histories with the lowest standard deviation of SA_{targ}/SA_{sim} and a mean value of SA_{targ}/SA_{sim} in the 0.5 to 2.0 range were retained for further analysis. To scale the records, a square root of the sum of the squares (SRSS) spectrum was constructed for each pair of horizontal ground motion components by taking the SRSS of the 5 percent damped response spectra for the scaled components. The same scaling factor was used for both components of a pair and each pair was scaled such that the average of the SRSS spectra from all horizontal component pairs fell above the NBCC 2010 spectrum for periods ranging from 0.2T to 1.5T, where T is the fundamental period of the structure. For each pair of motions, one component was selected to perform the nonlinear time history analysis of the two-dimensional model. The component that was chosen had the closest standard deviation between the scaled components compared to the standard deviation of the average of the SRSS spectra for periods ranging from 0.2T to 1.5T. The average spectrum from the seven selected scaled components also had to be equal to or exceed the NBCC 2010 spectrum for the period range from 0.2T to 1.5T; otherwise, an additional scaling factor had to be applied to all seven selected scaled components. The selected records and components are from the 1994 Northridge earthquake (TH01: Castaic Old Ridge Route, 360°, and TH02: Beverly Hills - 14145 Mulhol, 009°), 1989 Loma Prieta earthquake (TH05: Hollister - South & Pine, 090°, and TH07: Palo Alto - SLAC Lab, 270°), 1992 Landers earthquake (TH10: Barstow, 000°), 1971 San Fernando (TH12: Hollywood, 090°) and 1999 Hector Mine earthquake (TH19: Joshua Tree, 360°) and the final scaling factors for these records are, respectively: 1.485, 1.620, 1.485,

1.620, 1.755, 1.755 and 1.890. Figure 2 shows that the average of the SRSS spectra does not fall below the NBCC 2010 spectrum for periods ranging from 0.2T to 1.5T. However, the average spectrum of the seven selected components was below the NBCC 2010 spectrum and a second scaling factor had to be applied to all components to obtain the average spectrum of seven selected scaled components shown in Fig. 2.

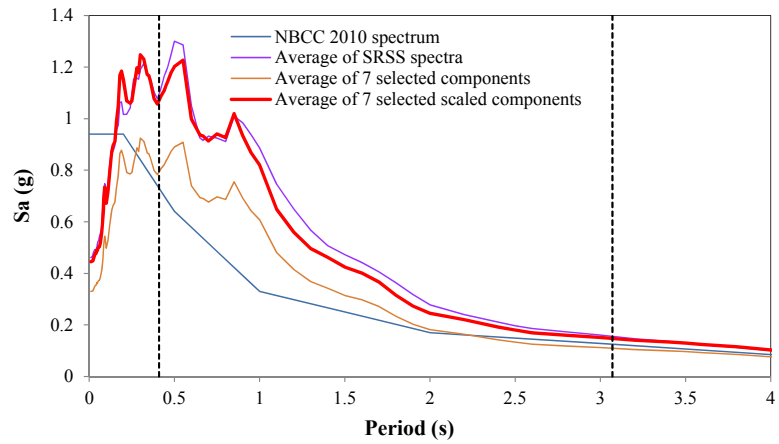

Figure 2. Scaling of the selected ground motions

ASSESSMENT RESULTS OF NONLINEAR ANALYSIS PROCEDURE

In the ASCE 41 standard, the axial tension and compression demands in braces are considered as deformation-controlled actions, and the acceptance criteria for the braces in the nonlinear procedure are expressed in terms of specific deformation limits. Braces are categorized as primary components and evaluated for the collapse prevention performance level. For braces in tension, the limit in ASCE 41 is $9\Delta_T$, where Δ_T is the axial deformation of the brace at the expected tensile yielding load. For the braces in compression, the acceptance criteria are $8\Delta_c$ and $7\Delta_c$ for slender and stocky compressive braces, respectively; where, Δ_c is the axial deformation of the brace at the expected buckling load. For the braces, the expected yield strength can be used and a value of 330 MPa was adopted. Results obtained for Model B were used to assess the elastic demand on beams, columns and brace connections. These components are considered as force-controlled. To evaluate beams and columns, the combined axial and flexural force demands were compared to the beam and column force capacities using the CSA S16-09 axial-bending interaction equations. The resistance factor was equal to 1.0 and the nominal yield strength was used to calculate the capacities. In Model C, inelastic buckling of the beams under axial and flexural demands was explicitly verified.

The results for one of the critical ground motions (TH02) are presented for models B and C. The time histories of the storey drift and axial force demands on the braces at the 1st floor obtained from Model B are illustrated in Figs. 3a and 3b, respectively. Large storey displacements developed at the 1st level as a consequence of buckling of the braces at that level. Buckling of the braces was accompanied by high brace axial deformation demand. Figure 3b shows that the strength of the brace connections in the 1st floor is attained and exceeded several times during the ground motion. In Fig. 3c, buckling of the braces at t = 5.2 s in the 1st level led to large flexural demand on the beam at that level. The axial load demand on the beam at the 1st floor exceeds the beam nominal compressive resistance, C_n, at t = 3.8 s, before buckling of the braces. Note that beam buckling was not modelled in Model B, and the axial load demand in the beam is compared to the beam nominal compressive resistance calculated assuming an effective length for in-plane buckling equal to the total beam length. Fig. 3d shows the evaluation of the right-hand side (RHS) column at the 1st floor. As shown, the axial load demand alone exceeds the column nominal axial strength, C_n. In addition, the large storey drift developing in the 1st level as a result of brace buckling induced high flexural demand on the columns at that level which would also likely contribute to column buckling.

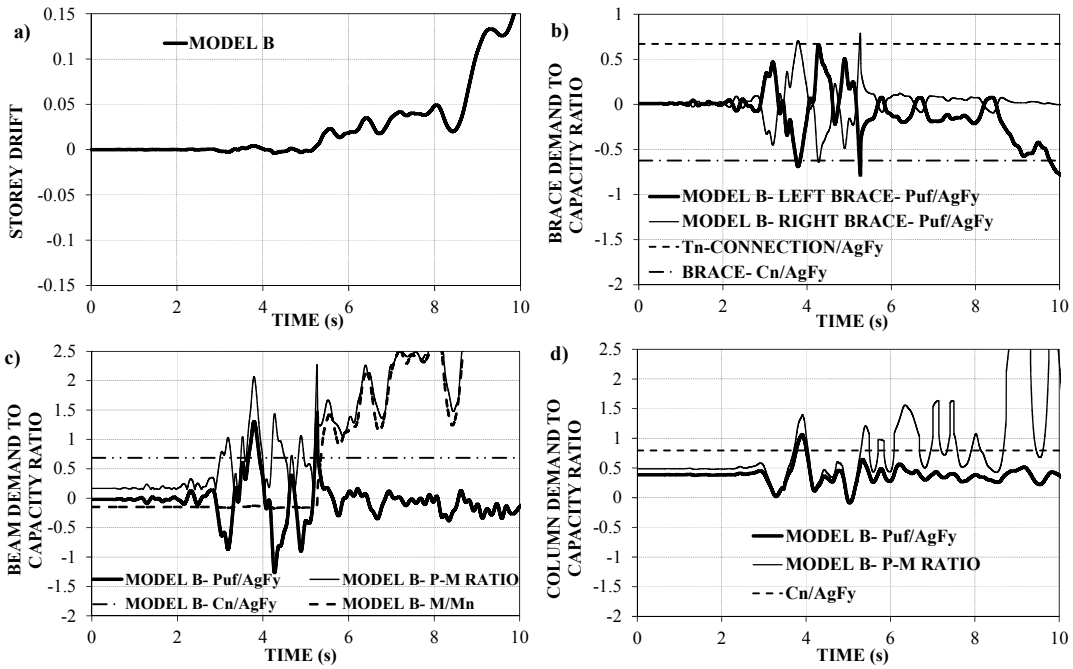

Figure 3. Response time history results from Model B under TH02: a) Storey drift at level 1; b) Brace axial force demand at level 1; c) Axial and flexural demands in the beam at level 1; and d) Axial and flexural demands in the column at level 1.

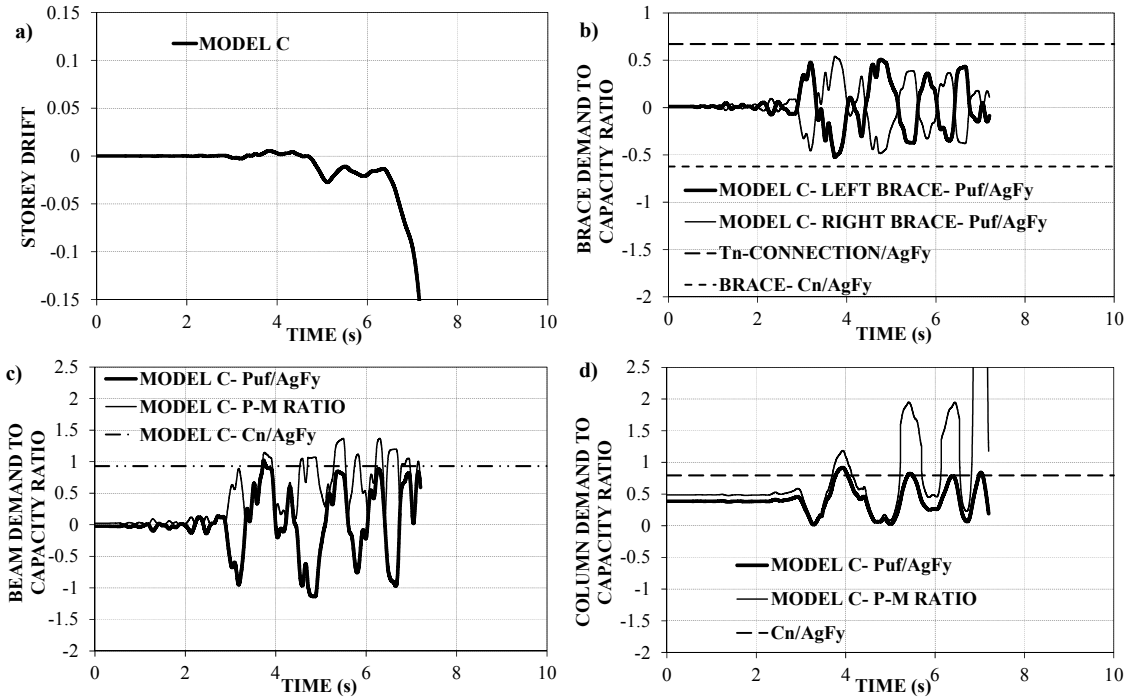

Figure 4. Response time history results from Model C under TH02: a) Storey drift at level 1; b) Brace axial force demand at level 1; c) Axial and flexural demands in the beam at level 1; and d) Axial and flexural demands in the column at level 1.

Figure 4 shows the time history response obtained under the same ground motion (TH02) when using Model C. In this model, beam buckling response was explicitly represented. In Fig. 4a, the storey displacement at level 1 is different from that shown in Fig. 3a because beam in-plane buckling occurred over half of the total beam length at that level, which affected the structure response. Figure 4b shows that brace buckling did not occur at the 1st floor and brace forces remained below the brace connection strength. This is because brace force demand was limited by beam buckling. In Fig. 4c, beam buckling is observed at the 1st storey at t = 3.8 s, when the axial load reached and slightly exceeded the beam C_n. Note that the beam C_n in this figure is calculated using an effective length equal to half of the total beam length because the braces did not buckle and could still offer a vertical support at the beam mid-length, which is consistent with the buckling mode observed in the analysis. Beam instability will be discussed in detail in the next section. Consistently with Model B, the axial load in the RHS column exceeded the nominal column compressive resistance (Fig. 4d). However, in Model C the flexural demand in the column was induced by the large drift caused by beam buckling. In the real structure, the presence of the floor slab would restrain the lateral displacement of the column at the 1st level. However, in general, the connection of beam to slab would have not been designed for that demand, and the retrofit strategy should be proposed to improve the seismic behaviour of the structure.

BEAM BUCKLING RESPONSE IN CHEVRON BRACED FRAME

Analyses with Model C revealed that in-plane beam buckling over half the beam length is a likely failure mode in steel chevron braced frames built prior to implementation of modern seismic design provisions, and it is typical for chevron braced frames with low gravity load on the beam. Beam buckling is therefore further investigated by conducting incremental static (pushover) analysis of the beam located at the 1st level of the 10-storey prototype building.

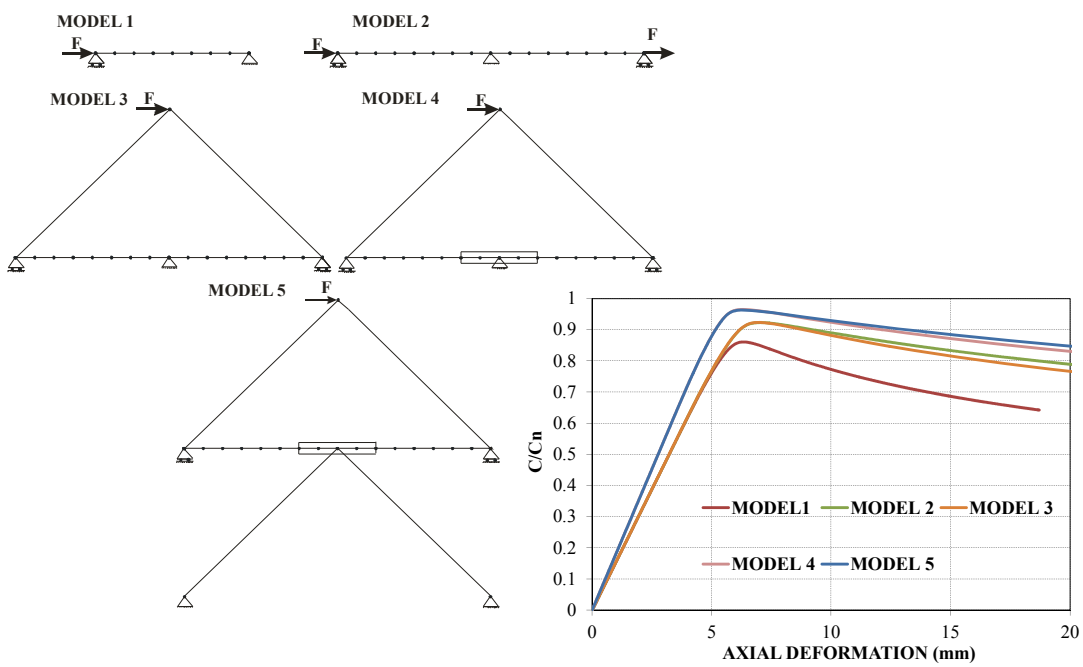

Figure 5. a) Models used for examination of the beam buckling response at the 1st level of chevron braced frame; and b) Computed beam axial load-deformation responses.

Five different models were considered to study in detail the beam buckling response and assess the beam compressive strength. The five models were developed by gradually including different

structural components, starting from a simple beam case represented in Model 1 to a 2-storey chevron braced frame assembly in Model 5 (Fig. 5a): Model 1 is a simple beam having half the beam length; Model 2 represents the continuous two-span beam; Model 3 includes the bracing members framing from above; Model 4 includes the gusset plate of the braces framing from below; and Model 5 includes the bracing members framing from below. In Models 3, 4 and 5, the braces were assumed to be pinned at their ends. In Models 1 and 2, axial loading was applied at one beam end. In subsequent models, beam axial load was induced by applying storey shear though the braces. Gravity loading was imposed on the beam. Figure 6 shows the location of the elements and the cross-section fiber discretization used for the beam in the different models.

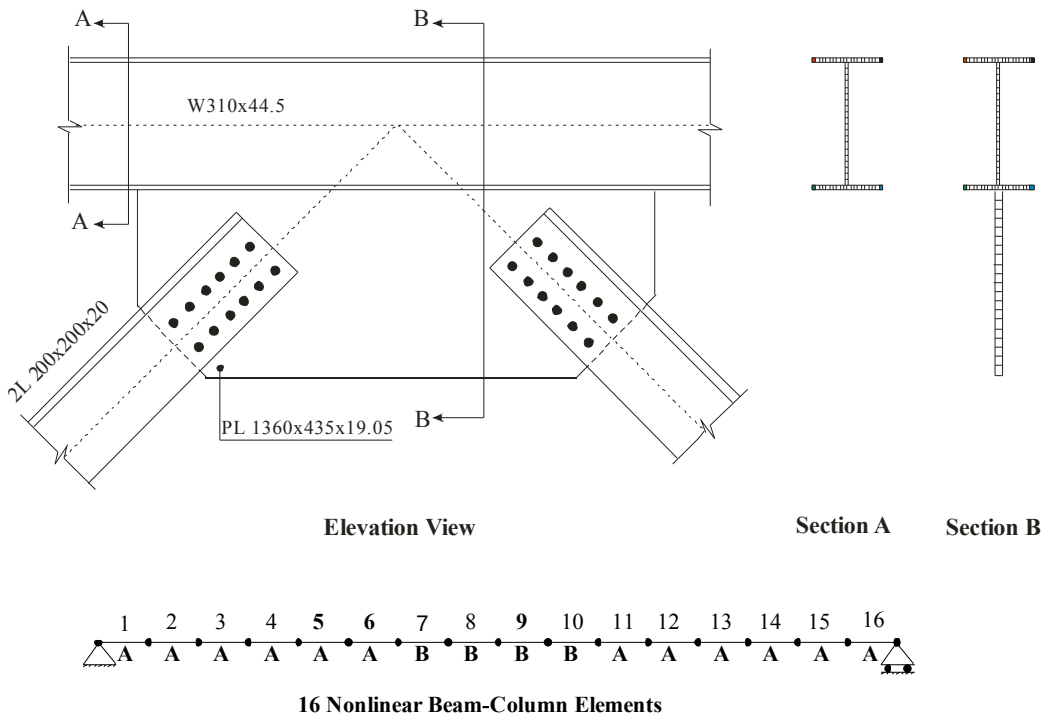

Figure 6. Location of elements and cross-section fibers in the beam member model

In Fig. 5b, the axial load-axial deformation responses of the compression half beam segment from the 5 different models are compared. In this figure, the beam C_n is determined with an effective length equal to half the chevron beam length. The peak C/C_n values from Models 1 to 5 are: 0.86, 0.923, 0.923, 0.964 and 0.963, respectively. The buckling strengths determined using Models 2 to 5 are higher than that obtained from Model 1. This could be expected because the additional flexural stiffness provided by the second half of the beam subjected to tension contributed to increase the buckling resistance of the compression half-beam segment. In Models 4 and 5, the presence of the gusset plate increased the beam axial and flexural stiffnesses; the latter also resulted in increased beam buckling strength. The results from the most representative Model 5 show that the C_n value from current code equations can be used to predict the beam buckling strength.

The evolution of the stresses and strains at the beam extreme top and bottom fibers upon beam buckling are presented for each model in Fig. 7. In Model 1, only the elements located in the left-hand side beam half-segment were included, and the results at the mid-length of the half-beam segment, i.e. at integration point 1 of element 5 were examined. Results at integration point 1 of element 9 were considered in Models 2 and 3, i.e. at the beam mid-length. In Models 4 and 5, the gusset plate extended over elements 7 to 10; therefore, the results at integration point 3 of element 6 were considered for these models.

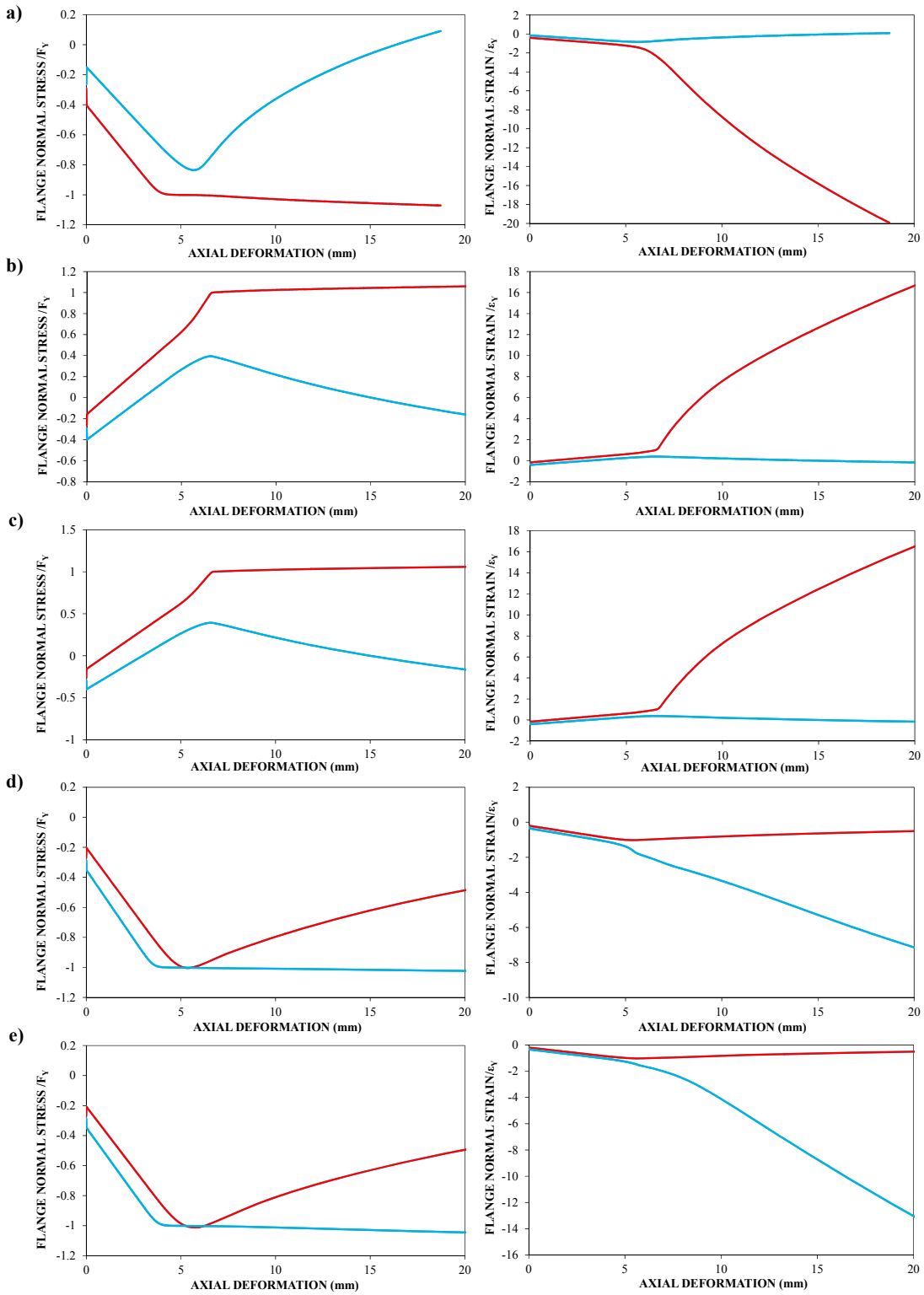

Figure 7. Stress and strain demands upon beam buckling from Models 1 (a) to 5 (e).

As seen in Fig. 7a, yielding in compression is reached in the fibers located at the beam top flange of Model 1, at an axial deformation of approximately 6 mm, when buckling occurred. Beyond that point, the variation of the stresses and strains in the bottom flanges is reversed as buckling deformations

increase. Figs. 7b and 7c show that the top flange fibers of Models 2 and 3 yield in tension at buckling of the beam. The presence of the braces framing from above has limited effects on the beam buckling response. In Models 4 and 5, yielding developed at the beam bottom flange, next to the gusset plate, when buckling occurred. The presence of the braces framing from below has limited impact on the stress and strain distributions before and after buckling.

CONCLUSIONS

The seismic performance of a steel tension-compression chevron braced frame used in a regular 10-storey building located in Vancouver, British Columbia, was assessed in accordance with the ASCE 41-13 standard. The structure was designed following the design provisions of the 1980 Canadian seismic code. Nonlinear time-history analyses were carried out for a set of seven ground motion records. The nonlinear analysis with brace nonlinear response showed the buckling of the braces at the first level, which led to large flexural demands on the beam at that level. The resulting large storey drift imposed bending moments on the columns and caused soft-storey response. The brace connections were also found to have insufficient capacity. When beam buckling was also represented in the nonlinear analysis, the beam at the first level buckled in-plane within its half-length, which caused large storey drifts and, thereby, high flexural demand on the columns. Beam buckling limited the axial forces that developed in the braces: the braces did not buckle at the first floor and the brace connection capacities were not reached. Further assessment of the beam buckling response in chevron braced frames was performed using five different beam models. The study showed that the beam in-plane buckling response and strength are influenced by the presence of the braces and the gusset plate connections, and the distribution of stresses and strains were sensitive to the modelling employed for braces and the gusset plates. Nevertheless, for this structure, the beam compressive strength could be predicted well by using current code equations assuming an effective length equal to the beam half-length.

ACKNOWLEDGEMENTS

The authors gratefully acknowledge the financial support provided by the Natural Sciences and Engineering Research Council of Canada (NSERC) for the Canadian Seismic Research Network (CSRN).

REFERENCES

ASCE (2013) Seismic evaluation and rehabilitation of existing buildings, ASCE/SEI 41-13 (Public Comment Draft), American Society of Civil Engineers, Reston, VA

Atkinson GM (2009) "Earthquake time histories compatible with the 2005 national building code of Canada uniform hazard spectrum", *Canadian Journal of Civil Engineering*, 36(6): 991-1000

Balazadeh-Minouei Y, Koboevic S, Tremblay R (2013) "Seismic evaluation of existing steel braced frames designed in accordance with the 1980 Canadian code requirements using nonlinear time history analysis", *In Proceedings of the CSCE 2013*, Montreal, Canada, May 29th - June 1st, Paper No. DIS-58

Bertero VV and Bozorgnia Y (2004) Earthquake Engineering from Engineering Seismology to Performance-Based Engineering, CRC Press LLC, Boca Raton, Florida, USA

CSA (1978) Limit states design of steel structures, CAN3 S16.1-M78, Canadian Standards Association, Toronto, ON

CSA (2009) Design of steel structures, CAN S16-09, Canadian Standards Association, Toronto, ON

Jiang Y, Tremblay R, Tirca L (2012) "Seismic assessment of deficient steel braced frames with built-up back-to-back double angle brace sections using OpenSees modelling", *In Proceedings of the 15WCEE*, Lisbon, Portugal, Paper No. 4416

Jiang Y, Balazadeh-Minouei Y, Tremblay R, Koboevic S, Tirca L (2012) "Seismic assessment of existing steel braced frames designed in accordance with the 1980 Canadian code provisions", In Behavior of Steel Structures in Seismic Area, *Proc. of the Seventh International Conference STESSA 2012*, Santiago, Chile, 531-537

McKenna F and Fenves GL (2004) Open System for Earthquake Engineering Simulation (OpenSees), Pacific Earthquake Engineering Research Center (PEER), University of California, Berkeley, CA (http://opensees.berkeley.edu/index.html)

Mitchel D, Paultre P, Tinawi R, Saatcioglu M, Tremblay R, Elwood K, Adams J, and DeVall R (2010) "Evolution of seismic design codes in Canada", *Canadian Journal of Civil Engineering*, 37(9):1157-1170

NRCC (2010, 1980) National building code of Canada, 2010, 13th Ed., 1980, 8th Ed., National Research Council of Canada, Ottawa, ON

Tremblay R (2011) "Evolution of the Canadian seismic design provisions for steel structures since 1989", *In Proceedings of the CSCE Annual Conference*, Ottawa, ON, 941-956